



# Primitive myxoid mesenchymal tumor of infancy with brain metastasis: first reported case

Amna Afzal Saeed<sup>1</sup> · Quratulain Riaz<sup>2</sup> · Nasir Ud Din<sup>3</sup> · Sadaf Altaf<sup>2</sup>

Received: 15 October 2017 / Accepted: 27 August 2018 / Published online: 3 September 2018  
© Springer-Verlag GmbH Germany, part of Springer Nature 2018

## Abstract

**Introduction** Primitive myxoid mesenchymal tumor of infancy (PMMTI) is a recently diagnosed entity, with only a handful of cases reported to date.

**Case description** Herein, we present the occurrence of this tumor in a 2-year-old boy, initially diagnosed as primitive neuroectodermal tumor of the extremity and treated with chemotherapy and surgical resection. He later presented with a cerebellar lesion, and biopsy was consistent with PMMTI.

**Conclusion** While there have been previous cases of PMMTI reported with loco-regional metastatic spread, to our knowledge, there is no known incidence of distant metastasis with involvement of the central nervous system, which makes this case the first of its kind.

**Keywords** Primitive myxoid mesenchymal tumor of infancy · Metastasis · Brain involvement

## Introduction

Primitive myxoid mesenchymal tumor of infancy (PMMTI) is a distinct soft tissue tumor, characterized by its positive reactivity to immunohistochemical markers such as CD99, CD117, and nestin, and a diffuse myxoid background with delicate vascularity on histopathology. Its treatment protocol mainly involves radical surgery. This tumor also has a tendency for local recurrences, if clear margins are not attained during resection. In this particular study, we present the first known PMMTI case with brain metastasis. The clinical and histopathological

description of the tumor, in addition to the chemical markers used as part of the diagnosis, has been reviewed below, along with the course of the disease and the management approach.

## Patient presentation and methods

A 2-year-old boy came to the clinic with a history of swelling on the medial aspect of the right arm since 1 month of age. An ultrasound was done which showed a well-defined hypoechoic structure in the upper part of the right arm, near the axilla with color flow on Doppler, suggestive of an enlarged lymph node. He was started on antibiotics and observed, but the swelling appeared to gradually increase in size. Consequently, an MRI contrast of the right arm was done which showed a large, well-defined, thin-walled collection in the anterior compartment of the right arm, displacing the surrounding muscles and vessels, showing fine septations, without any contrast enhancement, suggestive of a lymphangioma. Some of the images are given below in Fig. 1.

The patient underwent resection of the tumor. The histopathology report showed small tumor cells arranged in diffuse sheets. These tumor cells had small nuclei with clear to light eosinophilic cytoplasm. Myxoid changes were noted at the periphery, with interspersed scattered blood vessels. Immunohistochemical stain showed reactivity positive to

✉ Sadaf Altaf  
sadaf.altaf@aku.edu

Amna Afzal Saeed  
amna.afzal95@gmail.com

Quratulain Riaz  
quratulain.riaz@aku.edu

Nasir Ud Din  
nasir.uddin@aku.edu

<sup>1</sup> Medical College, Aga Khan University, Karachi, Pakistan

<sup>2</sup> Department of Pediatric Oncology, Aga Khan University Hospital, Karachi, Pakistan

<sup>3</sup> Department of Pathology and Laboratory Medicine, Aga Khan University Hospital, Karachi, Pakistan

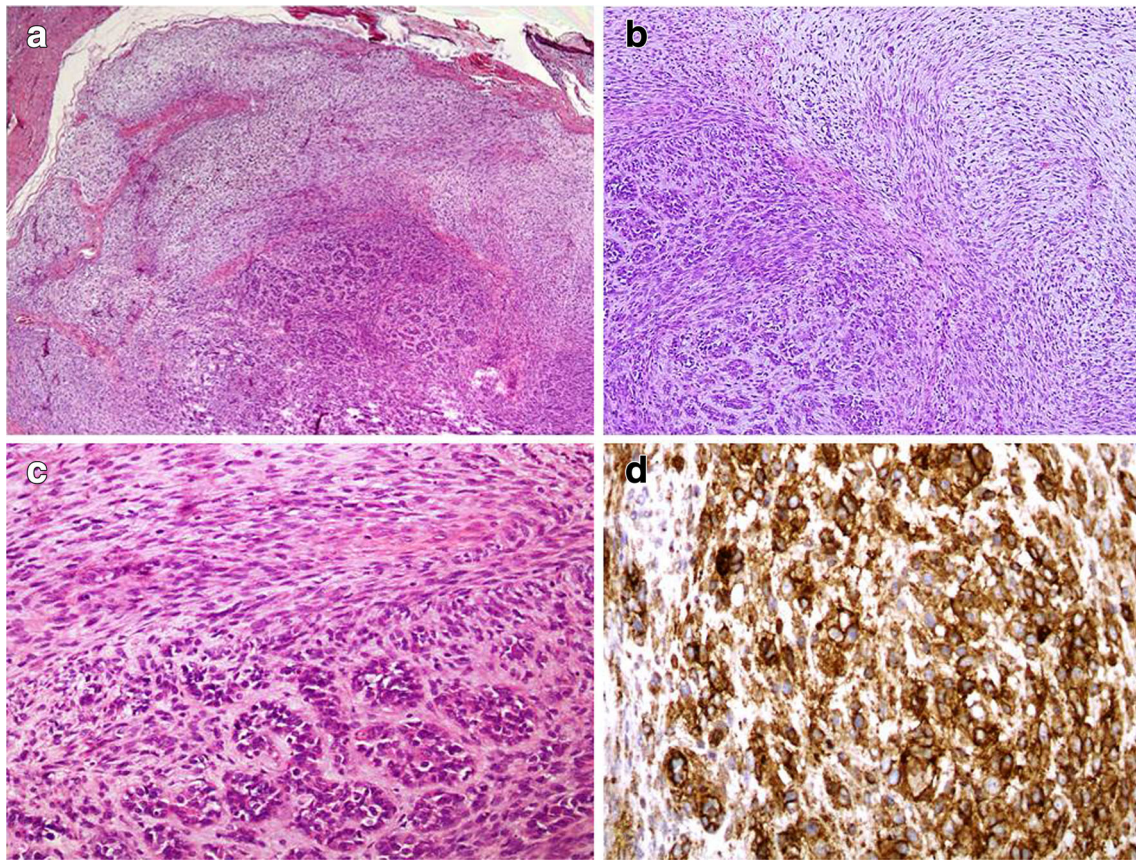


**Fig. 1** **a** Low power examination shows a lobulated tumor exhibiting primitive round and spindles cells present in a myxoid stroma. **b**, **c** Intermediated and high-power examination shows sharply demarcated

round and spindle cells. The round cells have hyperchromatic nuclei. **d** Membranous CD99 positivity in tumor cells

CD99, equivocal Myo-D1, and negative to desmin, myogenin, S-100, EMA, TdT, and synaptophysin. These findings suggested a primitive malignant round cell tumor, with differential diagnosis of Ewing sarcoma, owing to CD99 positivity. The metastatic work-up including bone scan, CT chest, and bone marrow aspirate was negative.

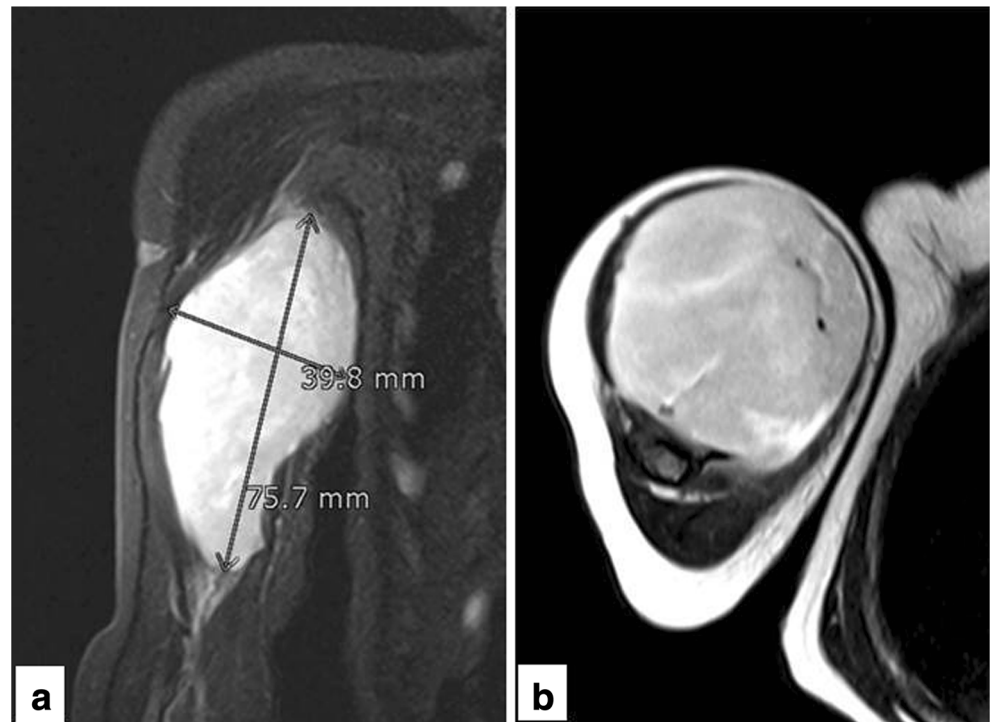
He was given six cycles of chemotherapy (vincristine, adriamycin, ifosfamide—VAI), followed by MRI which showed an interval reduction in tumor size and an overall improvement in the disease process. The child underwent re-resection and the histopathology showed no evidence of residual tumor. He received eight more cycles of chemotherapy, including VAI; however, the end-of-therapy MRI showed re-demonstration of well-defined elongated/ fusiform-shaped lesion within muscles along the anteromedial aspect of the right upper arm. He underwent re-resection and the histopathological findings that were reviewed at St. Jude Children's Research Hospital showed a partially circumscribed lesion with a nodular architecture, composed of short, oval spindle cells with moderate nuclear atypia arranged in sheets against a myxoid background, with a curvilinear vascular pattern. Focal areas show aggregates of round cells with vague tubule formation (Fig. 1a–c). Approximately 6–8 mitosis/10 HPF were

noted and the lesion was involving the inked excision margin. The tumor cells were negative for glycogen. Immunohistochemical staining was done which showed the cells were positive for CD99 and cyclin D1 (Fig. 1d) and negative for desmin, BCL6, SOX-10, CD34, S-100, EMA, cytokeratin, AE1/ AE3, smooth muscle actin (SMA), and alpha smooth muscle actin (ASMA). Molecular cytogenetics showed negativity for rearrangements of FUS and EWSR1 ruling out myxoid liposarcoma. These findings were consistent with low-grade primitive sarcoma of infancy (PMMTI).

Post-surgery MRI was repeated and few enhancing lymph nodes were identified in the right axilla. Additionally, there were enhancements identified along the neurovascular bundle in the axillary region. An abnormal signal intensity lesion was also identified on the anteromedial aspect of the lower metadiaphysis of the right humerus adjacent to the right brachialis. This was suspected to most likely represent residual/recurrent disease (Fig. 2a, b).

This was followed by a positron emission tomography (PET) scan, which showed bilateral fluorodeoxyglucose (FDG) avid level II and axillary lymph nodes with standardized uptake values (SUV) ranging up to 12.49 and few non-FDG avid hypodense regions in the right cerebellum,

**Fig. 2** Multi-planar T2 WI with and without fat saturation of the right shoulder showing a well-defined abnormal signal intensity mass in the anterior facial compartment of the right arm appearing hyperintense on T2-weighted images. No hemorrhage or significant contrast enhancement was noted within the mass or along its walls. Mass is displacing the surrounding muscles and vessels without any evidence of invasion or bone destruction



consistent with distant metastasis. MRI of the brain showed evidence of multiple focal lesions within the cerebellum on the right with extension down to the craniocervical junction. The lesions were hyper intense on T2-weighted images and fluid-attenuated inversion recovery (FLAIR) images, and hypo intense on T1-weighted images, with non-homogenous pattern of post-contrast enhancement, and likely representing metastatic involvement from the

previously diagnosed PMMTI (Fig. 3a, b). Histologically, tumor cells showed primitive round cells in myxoid stroma with focal spindle cells (Fig. 4a, b). Focal areas showed palisading of nuclei. Gross total resection of the disease was not possible due to proximity to the brain stem. Since chemotherapy or radiation therapy was also not an option, the family was counseled and it was mutually agreed to manage the child on palliation.

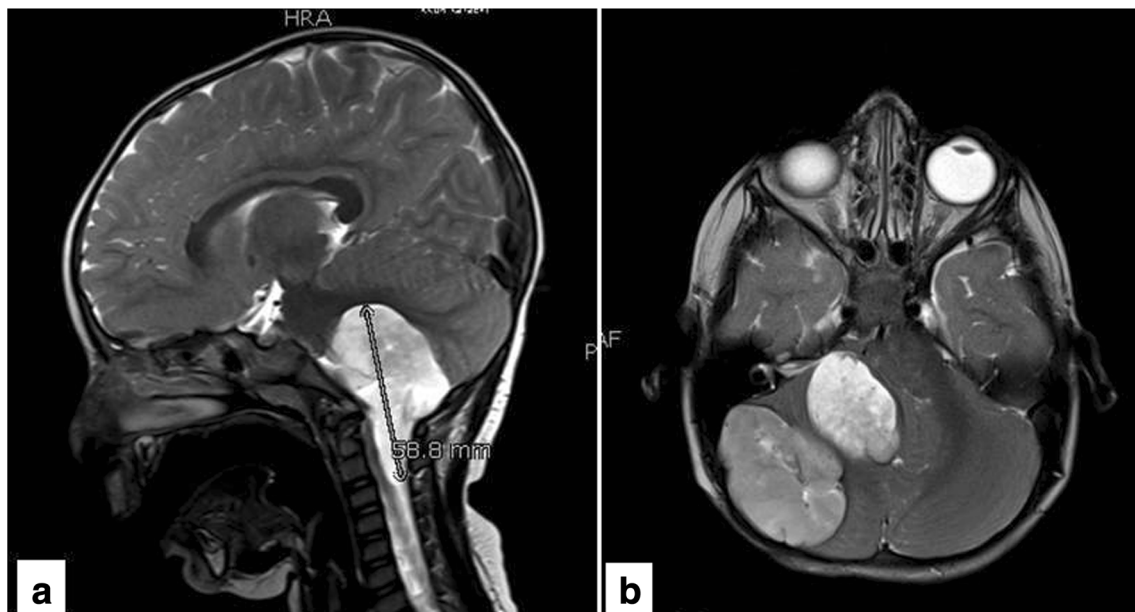


**Fig. 3** Multi-planar T2 WI showing multiple multi-lobulated abnormal signal intensity, likely extra axial lesions in the infratentorial compartment resulting in significant mass effect and displacement of the cerebellum, brainstem, and upper cervical cord

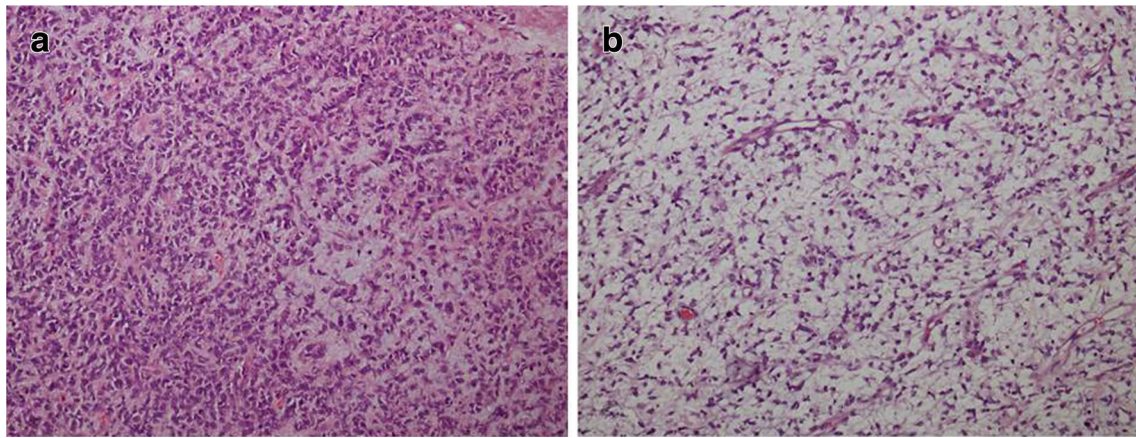


**Fig. 4** **a** Histology of metastatic tumor shows cords and nests of primitive round cells. **b** Spindle to round cells deposited in abundant myxoid stroma are noted in other areas of tumor

## Discussion

PMMTI is a rare soft tissue tumor that has been proven to be distinct from other tumors of infancy, on the basis of histopathology and immunohistochemical markers, and also on the nature of the tumor. It was first reported in 2006 by Alaggio et al., where he gave a clinic-pathologic report of six cases of PMMTI [1].

Microscopically, PMMTI usually has a diffuse myxoid background, delicate vascularity, small cystic spaces, low to moderate cellularity, increased atypia, and primitive mesenchymal tumor cells. One rare case also showed the presence of rosettes [2]. A study by Kao et al. has shown this feature of rosettes and small cell morphology to be associated with a more aggressive and poor prognosis. The tumor generally tends to range in size from 10 to 15 cm [3].

On immunohistochemistry, the tumor cells generally tend to show positive reactivity to CD99, CD117, and nestin, a positive or diffuse reactivity for vimentin, and negative reactivity to smooth muscle actin, muscle-specific actin, desmin, S-100 protein, or myogenin [4]. There is also no reactivity for myofibroblastic, myoid, or neural markers. Furthermore, internal tandem duplication of B cell CLL/lymphoma 6 (BCL6)-interacting co-repressor (BCOR) exon 15 and YWHAE-NUTM2B fusions have also been recently described to be present in PMMTI [5]. The presence of BCOR expression and YWHAE-NUTM2B fusions has also been noted in some soft tissue undifferentiated round cell sarcoma (URCS) and clear cell sarcoma of the kidney (CCSK). While there are overlapping morphological features of uniform round to spindle cells and it is proposed that there are similar genetic alterations among these tumors due to the clinicopathological overlap as well, PMMTI has shown to have a more prominent myxoid stroma. Therefore, even though the limits between PMMTI with URCS and PMMTI with CCSK are not so well defined, the characteristic histology of primitive cells with abundant myxoid stroma can help in better differentiating PMMTI from these tumors.

PMMTI is also different in its clinical nature, which includes early age at presentation, local recurrence, aggressiveness, and poor response to chemotherapy [6]. Commonly reported locations for this tumor include the somatic soft tissues of the trunk, the head and neck region, and the extremities [7]. However, distant metastases are rare. After Alaggio's initial report, another case series was written by Cuthbertson et al. This study included the cases reported by Alaggio and mentioned three additional ones too. From these nine verified cases, all but two recurred. There were no distant metastases, and only one patient died of the disease. Furthermore, in all but one of these nine cases, the tumor presented itself at an early age, with the odd one occurring in a child (non-infant) at the age of 3. In all of these patients, surgery was performed to remove the tumor, with chemotherapy being used in just three cases [8]. It is also notable that with all the three cases where chemotherapy was used, recurrences eventually occurred.

Recently, five more cases were reported by Santiago et al. These consisted of three girls and two boys with mean age of 6.5 months. The tumors were located in the paraspinal region ( $n = 3$ ), back ( $n = 1$ ), or foot ( $n = 1$ ) and ranged in size from 2.5 to 10.2 cm. In all five cases, BCOR internal tandem duplication was confirmed via PCR and sequencing [9]. For our patient, BCOR immunohistochemical staining and FISH analysis for ETV6-NTRK3 rearrangement were not performed as it is not available in our lab. Cyclin D1 and BCL6 molecular analysis was performed. Cyclin D1 was positive and BCL6 was negative.

The tumors in the differential diagnosis of PMMTIs include embryonal rhabdomyosarcoma, Ewing sarcoma/primitive neuroectodermal tumor, congenital infantile fibrosarcoma (CIF), and primitive sarcomas such as undifferentiated sarcoma. The absence of BCOR and BCL6 immunoreactivity in CIF further helps to differentiate it from PMMTI, on the basis of molecular techniques and also further points out how PMMTI is entirely different from other soft tissue sarcomas. Another diagnostic modality would be CT or MRI,

where PMMTI will likely show prominent vascularity but little contrast enhancement [10].

The increased attention given to differentiating PMMTI from other tumors of similar nature is primarily because of its different management approach. Because PMMTI is already a rare entity and the tumors have been variously diagnosed and treated, it is difficult to define the best options with regard to management. So far, the preferred mode of treatment is radical surgical excision with establishment of negative margins [11]. This may require partial amputations or extensive dissections creating large and morbid defects. Ensuring negative margins during surgical excision is

imperative as the most notable risk factor for local recurrence is excision without negative margins, where recurrences usually tend to occur within months. Because this tumor is unresponsive to chemotherapy, treatment of primary tumors and recurrences can get difficult. To date, radiation therapy has not been implemented as a sole treatment modality and the long-term outcome for these patients is unclear. For instance, one case report showed the unusual transformation of a PMMTI into an undifferentiated high-grade sarcoma, 5 years after surgical resection of the primary PMMTI [12]. Table 1 shows the clinical course and treatment of published cases on PMMTI.

**Table 1** Table of published cases with clinical course

Author	Sex	Age	Location of tumor	Size of tumor (cm)	Treatment	Recurrence	Outcome (on follow-up from available records)
Alaggio 2006	Male	15 days	Larynx	2.5	Surgery, chemotherapy	Yes	Alive with disease
Alaggio 2006	Male	1 month	Thigh	15	Surgery, chemotherapy	Yes	No evidence of disease
Alaggio 2006	Male	2 months	Forearm	10	Surgery	None	No evidence of disease
Alaggio 2006	Male	2 months	Paraspinal soft tissue	5.5	Surgery	Unknown	Unavailable
Alaggio 2006	Female	Newborn	Supraclavicular soft tissue	5	Surgery	Yes	Alive with disease
Alaggio 2006	Female	Newborn	Back, chest, neck, abdomen	15	Surgery	Residual disease	Dead with disease
Mulligan 2011	Female	8 months	Thenar eminence	2	Surgery	Yes	No evidence of disease
Lam 2011 [13]	Male	3 months	Back	3.5	Surgery	None	No evidence of disease
Gong 2012	Male	5 months	Anterior neck soft tissue	4.5	Surgery	Yes	Alive with disease
Gong 2012	Female	Newborn	Dorsal lumbar region	6	Surgery	Yes	U/A
Su TC 2013	Male	3 months	Scalp	N/A	Surgery	None	No evidence of disease
Saito 2013	Female	19 months	Sacrococcygeal	4.5	Surgery	None	No evidence of disease
Cuthbertson 2014	Female	3 years	Hard palate	7	Surgery, chemotherapy	Yes	No evidence of disease
Wang 2014	Male	4 years	Head and neck ( $n = 2$ )	N/A	Surgery	1 patient had local recurrences twice and died 2 years later. Other 2 remained well with no evidence of disease.	
Wang 2014	Male	2 days	and lumbar	N/A	Surgery		
Wang 2014	Female	3 months	region ( $n = 1$ )	N/A	Surgery		
Cipriani 2014	Female	15 months	Ankle	2	Excisional biopsy	None	No evidence of disease
Guilbert 2015	Female	8 months	Cervical mass	7.5	Surgery, chemotherapy	Yes	Alive with disease
Foster 2016	Female	3 months	Upper chest wall	7	Surgery	No	No evidence of disease
Cramer 2017 [14]	Female	13 months	Paraspinal mass	0.8	Surgery, chemotherapy, radiation	Yes	No evidence of disease
Kao 2017	Male	9 months	Abdominal wall	N/A	N/A	Yes	Alive with disease
Kao 2017	Male	6 months	Retroperitoneum	N/A	N/A	N/A	N/A
Kao 2017	Female	10 months	Abdominal cavity	N/A	N/A	N/A	N/A
Kao 2017	Female	4 months	Paravertebral	N/A	N/A	N/A	N/A
Kao 2017	Male	1 year	Thigh	N/A	N/A	N/A	N/A
Santiago 2017	Male	1 week	Paraspinal	10.5	N/A	N/A	N/A
Santiago 2017	Female	9 months	Back	2.5	N/A	N/A	N/A
Santiago 2017	Female	8 months	Paraspinal	N/A	N/A	N/A	N/A
Santiago 2017	Female	13 months	Paraspinal	N/A	N/A	N/A	N/A
Santiago 2017	Male	2 months	Left foot	3.4	N/A	N/A	N/A
Present case	Male	2 years	Medial aspect of arm	7.8	Surgery, chemotherapy	Yes	No follow-up

N/A not available

This report presents a child who had PMMTI with distant metastasis to the brain. To our knowledge, this is the first reported case of a PMMTI with such a clinical course. This study, and others on PMMTI, emphasizes the importance of cytogenetics and testing of molecular markers and immunohistochemical techniques in the diagnosis of these soft tissue sarcomas [15].

**Acknowledgements** The authors acknowledge the pathologists of St. Jude Children's Research Hospital for reviewing the slides and performing molecular studies.

### Compliance with ethical standards

**Conflict of interest** On behalf of all authors, the corresponding author states that there is no conflict of interest.

### References

- Alaggio R, Ninfo V, Rosolen A, Coffin CM (2006) Primitive myxoid mesenchymal tumor of infancy: a clinicopathologic report of 6 cases. *Am J Surg Pathol* 30(3):388–394
- Cipriani NA, Ryan DP, Nielsen GP (2014) Primitive myxoid mesenchymal tumor of infancy with rosettes: a new finding and literature review. *Int J Surg Pathol* 22(7):647–651
- Su TC, Hwang MJ, Li CF, Wang SC, Lee CH, Chen CJ (2013) A rare malignant tumor of scalp in a 3-month-old Taiwanese infancy: case report of primitive myxoid mesenchymal tumor of infancy with molecular study. *Med Mol Morphol* 46(2):109–113
- Gong Q, Wang Z, Li X, Fan Q (2012) Primitive myxoid mesenchymal tumor of infancy: report of two cases and review of the literature. *Pathol Int* 62(8):549–553
- Kao YC, Sung YS, Zhang L, Huang SC, Argani P, Chung CT, Graf NS, Wright DC, Kellie SJ, Agaram NP, Ludwig K, Zin A, Alaggio R, Antonescu CR (2016) Recurrent BCOR internal tandem duplication and YWHAE-NUTM2B fusions in soft tissue undifferentiated round cell sarcoma of infancy: overlapping genetic features with clear cell sarcoma of kidney. *Am J Surg Pathol* 40(8):1009–1020
- Mulligan L, O'meara A, Orr D et al (2010) Primitive myxoid mesenchymal tumor of infancy: a report of a further case with locally aggressive behavior. *Pediatr Dev Pathol* 14(1):75–79
- Wang H, Liu Q, Wang J et al (2014) Primitive myxoid mesenchymal tumor of infancy: a clinicopathologic study of 3 additional cases. *Zhonghua Bing Li Xue Za Zhi* 43(6):375–378
- Cuthbertson DW, Caceres K, Hicks J et al (2014) A cooperative approach to diagnosis of rare diseases: primitive myxoid mesenchymal tumor of infancy. *Ann Clin Lab Sci* 44(3):310–316
- Santiago T, Clay MR, Allen SJ, Orr BA (2017) Recurrent BCOR internal tandem duplication and BCOR or BCL6 expression distinguish primitive myxoid mesenchymal tumor of infancy from congenital infantile fibrosarcoma. *Mod Pathol* 30(6):884–891
- Saito A, Taketani T, Kanai R, Kanagawa T, Kumori K, Yamamoto N, Ishikawa N, Takita J, Yamaguchi S (2013) A case with sacrococcygeal primitive myxoid mesenchymal tumor of infancy: a case report and review of the literature. *J Pediatr Hematol Oncol* 35(7):e280–e282
- Foster JH, Vasudevan SA, Hicks MJ, Schady D, Chintagumpala M (2016) Primitive myxoid mesenchymal tumor of infancy involving chest wall in an infant: a case report and clinicopathologic correlation. *Pediatr Dev Pathol* 19(3):244–248
- Guilbert MC, Rougemont AL, Samson Y, Mac-Thiong JM, Fournet JC, Soglio DBD (2015) Transformation of a primitive myxoid mesenchymal tumor of infancy to an undifferentiated sarcoma: a first reported case. *J Pediatr Hematol Oncol* 37(2):e118–e120
- Lam J, Lara-Corrales I, Cammisuli S et al (2010) Primitive myxoid mesenchymal tumor of infancy in a preterm infant. *Pediatr Dermatol* 27:635–637
- Cramer SL, Li R, Ali S, Bradley JA, Kim HK, Pressey JG (2017) Successful treatment of recurrent primitive myxoid mesenchymal tumor of infancy with BCOR internal tandem duplication. *J Natl Compr Cancer Netw* 15(7):868–871
- Warren M, Turpin BK, Mark M, Smolarek TA, Li X (2016) Undifferentiated myxoid lipoblastoma with PLAG1–HAS2 fusion in an infant; morphologically mimicking primitive myxoid mesenchymal tumor of infancy (PMMTI)—diagnostic importance of cytogenetic and molecular testing and literature review. *Cancer Genet* 209(1):21–29